

From One-Trick Ponies to All-Rounders: On-Demand Learning for Image Restoration

Ruohan Gao and Kristen Grauman
University of Texas at Austin
{rhgao, grauman}@cs.utexas.edu

Abstract

While machine learning approaches to image restoration offer great promise, current methods risk training “one-trick ponies” that perform well only for image corruption of a particular level of difficulty—such as a certain level of noise or blur. First, we expose the weakness of today’s one-trick pony and demonstrate that training general models equipped to handle arbitrary levels of corruption is indeed non-trivial. Then, we propose an on-demand learning algorithm for training image restoration models with deep convolutional neural networks. The main idea is to exploit a feedback mechanism to self-generate training instances where they are needed most, thereby learning models that can generalize across difficulty levels. On four restoration tasks—image inpainting, pixel interpolation, image deblurring, and image denoising—and three diverse datasets, our approach consistently outperforms both the status quo training procedure and curriculum learning alternatives.

1. Introduction

Deep convolutional networks [20, 35, 12] have swept the field of computer vision and have produced stellar results on various recognition benchmarks in the past several years. Recently, deep learning methods are also becoming a popular choice to solve low-level vision tasks in image restoration, with exciting results [6, 25, 22, 45, 4, 16, 30, 43]. Restoration tasks such as image super-resolution, inpainting, deconvolution, matting, and colorization have a wide range of compelling applications. For example, deblurring techniques can be used to remove blurring artifacts from photos caused by motion blur or defocus aberration; colorization methods can hallucinate a plausible color version of an old grayscale photograph; denoising methods can recover digital images corrupted by sensor noise due to poor illumination, high temperature, or transmission errors.

A learning-based approach to image restoration enjoys the convenience of being able to *self-generate* training in-

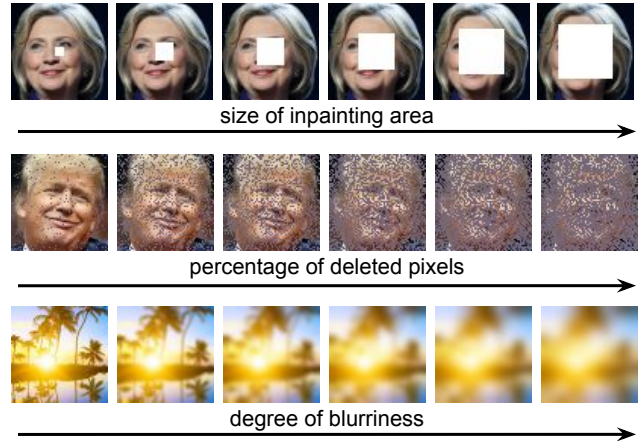


Figure 1. Illustration of three image restoration tasks: image inpainting, pixel interpolation, and image deblurring. Each task can be divided into sub-tasks of increasing difficulty (from left to right). Our work aims to train an “all-rounder” model that performs well across the spectrum of difficulty for each task.

stances purely based on the original real images. Whereas training an object recognition system entails collecting images manually labeled with object categories by human annotators, an image restoration system can be trained with arbitrary, synthetically corrupted images. The original image itself is the ground-truth the system learns to recover.

While existing methods take advantage of this convenience, they typically do so in a problematic way. Image corruption exists in various degrees of severity, and so in real-world applications the difficulty of restoring images will also vary significantly. For example, as shown in Fig. 1, an inpainter may face images with varying sizes of missing content, and a deblurring system may encounter varying levels of blurriness. Intuitively, the more missing pixels or the more severe the blur, the more difficult the restoration task. However, the norm in existing deep learning methods is to train a model that succeeds at restoring images exhibiting *a particular level of corruption difficulty*. In particular, existing systems self-generate training instances with a

manually fixed hyper-parameter that controls the degree of corruption—a fixed inpainting size [30, 43], a fixed percentage of corrupted pixels [43, 25], or a fixed level of Gaussian white noise [25, 40, 15, 3]. The implicit assumption is that at test time, either i) corruption will be limited to that same difficulty, or ii) some other process will estimate the difficulty level before passing the image to the appropriate, separately trained restoration system. Unfortunately, these are strong assumptions that are difficult if not impossible to meet in practice. As a result, existing methods risk being “one-trick ponies”. Deep networks can severely overfit to a certain degree of corruption. Taking the inpainting task as an example, a well-trained deep network may be able to inpaint a 32×32 block out of a 64×64 image very well, then fail miserably at inpainting a (seemingly easier) 10×10 block (see Fig. 2 and Sec. 4).

How should we train an image restoration system to be an “all-rounder”—to succeed across a spectrum of difficulty levels? To consider the alternatives, imagine the following scenario. Alice, Bob, Charlie, and David all study at CVPR Elementary School. Every week, they get the same assignments from their teachers. Alice is arrogant, and she only completes the most difficult questions and thinks that answering other questions is a waste of her time. Bob is lazy and unambitious, and he only completes the easy questions. Charlie is dutiful, and he always completes all the questions exactly as required. David is similar to Charlie, but not only does he complete all the questions, he also reflects on his mistakes after he gets each of the graded assignments. Whenever he finds that he often has trouble with some type of questions, he spends more quality time tackling other problems like them. In the final exam at the end of the semester, who do you think will get the highest mark among the four of them?

Conscious of this analogy in human learning, in this work we explore ways to let a deep learning system take control and guide its own training. This includes i) a solution that simply pools training instances from across difficulty levels, ii) a solution that focuses on hard examples, and iii) a curriculum learning solution that intelligently orders the training samples from easy to hard. Based on our findings, we introduce a new *on-demand learning* solution for training all-rounder deep networks for image restoration tasks. Our approach relies on a feedback mechanism that, at each epoch of training, lets the system guide its own learning towards the right proportion of sub-tasks per difficulty level. In this way, the system itself can discover which sub-tasks deserve more or less attention.

To implement our idea, we devise a general encoder-decoder network amenable to several restoration tasks. We evaluate the approach on four low-level tasks—inpainting, pixel interpolation, image deblurring and image denoising—and three diverse datasets, CelebFaces At-

tributes [26], SUN397 Scenes [39], and Denoising Benchmark 11 (DB11) [5, 3]. Across all tasks and datasets, the results consistently demonstrate the advantage of our proposed method. On-demand learning helps avoid the common (but thus far overlooked) pitfall of overly specializing deep networks to a narrow band of distortion difficulty.

2. Related Work

Deep Learning in Low-Level Vision: Deep learning for image restoration is on the rise. Vincent *et al.* [37] propose one of the most well-known models: the stacked denoising auto-encoder. A multi-layer perceptron (MLP) is applied to image denoising by Burger *et al.* [3] and post-deblurring denoising by Schuler *et al.* [34]. Convolutional neural networks are also applied to natural image denoising [15] and used to remove noisy patterns (e.g., dirt/rain) [8]. Apart from denoising, deep learning is gaining traction for various other low-level tasks: super-resolution [6, 16], inpainting [30, 43], deconvolution [42], matting [4], and colorization [22, 45]. While many models specialize the architecture towards one restoration task, recent work by Liu *et al.* presents a unified network for multiple tasks [25]. Our encoder-decoder pipeline also applies across tasks, and serves as a good testbed for our main contribution—the idea of on-demand learning. Our idea has the potential to benefit any existing method currently limited to training with a narrow band of difficulty [30, 43, 15, 3, 34, 25].

The one-trick pony problem is also observed in recent denoising work, e.g., [3, 29], but without a dedicated and general solution. Burger *et al.* [3] attempt to train a network on patches corrupted by noise with different noise levels by giving the noise hyper-parameter as an additional input to the network. While the model can better denoise images at different noise levels, assuming the noise level is known at test time is problematic. Recently, Mao *et al.* [29] explore how the large capacity of a very deep network can help generalize across noise levels, but accuracy still declines noticeably from the one-trick counterpart.

Curriculum and Self-Paced Learning: Training neural networks according to a *curriculum* can be traced back at least to Elman [10]. The basic idea is that successful learning may depend on starting small, learning easier aspects of the task and then gradually increasing the difficulty level. Prior work on curriculum learning mainly focuses on supervised learning and a single task, like the seminal work of Bengio *et al.* [2]. The curriculum consists of a manually-supplied ordering of training examples, from easy to difficult. Recently, Pentina *et al.* [31] pose curriculum learning in a multi-task learning setting, where sharing occurs only between subsequent tasks. Building on the curriculum concept, in *self-paced* learning, the system *automatically* chooses the order in which training examples are processed. Kumar *et al.* [21] and Lee *et al.* [23] present self-paced al-

gorithms for object detection. We are not aware of any prior work in curriculum/self-paced learning that deals with image restoration. Like self-paced learning, our approach does not rely on human annotations to rank training examples from easiest to hardest. Unlike self-paced work, however, our on-demand approach self-generates training instances of a targeted difficulty.

Active Learning: Active learning is another way for a learner to steer its own learning. Active learning selects examples that seem most valuable for human labeling, and has been widely used in computer vision to mitigate manual annotation costs [18, 13, 9, 36, 24, 11, 17, 38]. Unlike active learning, our approach uses no human annotation, but instead actively synthesizes training instances of different corruption levels based on the progress of training. All our training data can be obtained for “free” and the ground-truth (original uncorrupted image) is always available.

3. Roadmap

We first examine the one-trick pony problem, and provide concrete evidence that it hinders deep learning for image restoration (Sec. 4). Then we present a unified view of image restoration as a learning problem (Sec. 5.1) and describe inpainting, interpolation, and deblurring as instantiations (Sec. 5.2). Next we introduce the on-demand learning idea (Sec. 5.3) and a network architecture to implement it (Sec. 5.4). Finally, we present results (Sec. 6).

4. The One-Trick Pony Problem

The one-trick pony problem arises when existing image restoration methods train a learning algorithm to restore images with a controlled degree of corruption [40, 43, 3, 34, 30, 25]. For example, Yeh *et al.* [43] train an image inpainter at a fixed size and location, and always delete 80% of pixels for pixel interpolation. Pathak *et al.* [30] mainly focus on a large central block for the inpainting task. Liu *et al.* [25] solve denoising, pixel interpolation, and color interpolation tasks all with a restricted degree of corruption.

Just how bad is the one-trick pony in image restoration tasks? Fig. 2 helps illustrate. To get these results, we followed the current literature to train deep networks to target a certain degree of corruption for three applications.¹

Specifically, **for the image inpainting task**, following similar settings of prior work [30, 43], we train a model to inpaint a large central missing block of size 32×32 . During testing, the resulting model can inpaint the central block of the same size at the same location very well (first row in Fig. 2-a). However, if we remove a block that is slightly shifted away from the central region, or remove a much *smaller* block, the model fails to inpaint satisfactorily

¹See Sec. 6 for quantitative results, and Sec. 5.4 for details about the encoder-decoder network used.

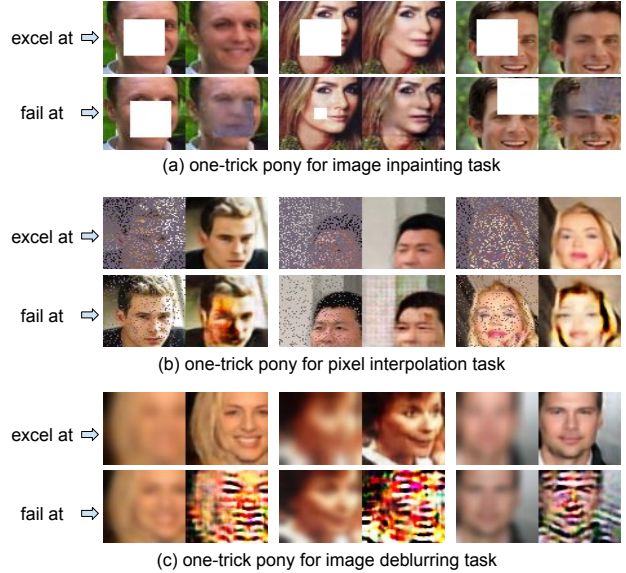


Figure 2. Illustration of the severity of overfitting for image inpainting, pixel interpolation, and image deblurring tasks. The models overfit to a certain degree of corruption. They perform extremely well at that level of corruption, yet fail to produce satisfactory restoration results even for much easier sub-tasks.

(second row in Fig. 2-a). Following [30], we replace pixels in removed blocks with the average pixel values in training images (which tend to look grey). We can observe that grey areas are retained in regions outside of the central block in the failure cases, which is a strong indicator that the trained network severely overfits to the central location.

For the pixel interpolation task, we train a model only based on heavily corrupted images (80% of random pixels deleted), following [43]. During testing, if we use the obtained model to restore images of the same corruption level, the images are recovered very well (first row in Fig. 2-b). However, if we test the same model on *lightly* corrupted (easier) images, the model performs very poorly (second row in Fig. 2-b). The trained network either produces common artifacts of deep networks like the checkerboard artifacts, or a much blurrier low-quality restored image.

For the image deblurring task, results are similar. We train a model only based on heavily blurred images ($\sigma_x = \sigma_y = 5$). The trained model can successfully restore very blurry images (same blurry level as training examples), but is unable to restore images that are much less blurry. In the second row of Fig. 2-c, we can observe some ripple artifacts, which may be similar to the shape of the Gaussian kernel function that the network overfits to.

More examples of One-Trick Ponies for the three tasks are shown in Fig. 9. The details of the deep networks used to generate the results in Fig. 2 and Fig. 9 are not identical to those in prior work. However, we stress that the limitation in their design that we wish to highlight is orthogonal to

the particular architecture. To apply them satisfactorily in a general manner would require training a separate model for each hyper-parameter. Even if one could do so, it is difficult to gauge the corruption level in a novel image and decide which model to use. Finally, as we will see below, simply pooling training instances across all difficulty levels is also inadequate.

5. Approach

Next we present ideas for overcoming the one-trick pony.

5.1. Problem Formulation

While the problem of overfitting is certainly not limited to image restoration, both the issue we have exposed as well as our proposed solution are driven by its special ability to self-generate “free” training instances under specified corruption parameters. Recall that a real training image automatically serves as the ground-truth; the corrupted image is synthesized by applying a randomized corruption function.

We denote a real image as \mathcal{R} and a corrupted image as \mathcal{C} (e.g., a random block is missing, some percentage of random pixels are deleted, or the whole image is blurred). We model their joint probability distribution by $p(\mathcal{R}, \mathcal{C}) = p(\mathcal{R})p(\mathcal{C}|\mathcal{R})$, where $p(\mathcal{R})$ is the distribution of real images and $p(\mathcal{C}|\mathcal{R})$ is the distribution of corrupted images given the original real image. In the case of a one-trick pony, \mathcal{C} may be a deterministic function of \mathcal{R} (e.g., specific blur kernel).

To restore the corrupted image, the most direct way is to find $p(\mathcal{R}|\mathcal{C})$ by applying Bayes’ theorem. However, this is not feasible because $p(\mathcal{R})$ is intractable. Therefore, we resort to a point estimate $f(\mathcal{C}, \mathbf{w})$ through an encoder-decoder style deep network (**details in Sec. 5.4**) by minimizing the following mean squared error objective:

$$\mathbb{E}_{\mathcal{R}, \mathcal{C}} \|\mathcal{R} - f(\mathcal{C}, \mathbf{w})\|_2^2.$$

Given a corrupted image \mathcal{C}_0 , the minimizer of the above objective is the conditional expectation: $\mathbb{E}_{\mathcal{R}}[\mathcal{R}|\mathcal{C} = \mathcal{C}_0]$, which is the average of all possible real images that could have produced the given corrupted image \mathcal{C}_0 .

Denote the set of real images $\{\mathcal{R}_i\}$. We synthesize corrupted images $\{\mathcal{C}_i\}$ correspondingly to produce training image pairs $\{\mathcal{R}_i, \mathcal{C}_i\}$. We train our deep network to learn its weights \mathbf{w} by minimizing the following Monte-Carlo estimate of the mean squared error objective:

$$\hat{\mathbf{w}} = \underset{\mathbf{w}}{\operatorname{argmin}} \sum_i \|\mathcal{R}_i - f(\mathcal{C}_i, \mathbf{w})\|_2^2.$$

During testing, our trained deep network takes a corrupted image \mathcal{C} as input and forwards it through the network to output $f(\mathcal{C}, \mathbf{w})$ as the restored image.

5.2. Image Restoration Task Descriptions

Under this umbrella of a general image restoration solution, we consider three tasks.

Image Inpainting The image inpainting task aims to re-fill a missing region and reconstruct the real image \mathcal{R} of an incomplete corrupted image \mathcal{C} (e.g., with a contiguous set of pixels removed). In applications, the “cut out” part of the image would represent an occlusion, cracks in photographs, or an object that should be removed from the photo. Whereas [30, 43] focus on inpainting a large missing block of a certain size in the central region of the image, we make the missing square block randomized across the whole image in both position and scale.

Pixel Interpolation Related to image inpainting, pixel interpolation aims to refill non-contiguous deleted pixels. The system reconstructs the real image \mathcal{R} from a corrupted image \mathcal{C} in which a certain percentage of pixels are removed. The network has to reason about the image structure and infer values of the deleted pixels by interpolating from neighboring pixels. Applications include more fine-grained inpainting tasks such as removing dust spots in film.

Image Deblurring The image deblurring task aims to remove the blurring effects of a corrupted image \mathcal{C} to restore the corresponding real image \mathcal{R} . We use Gaussian smoothing to blur a real image to create training examples. The kernel’s horizontal and vertical widths (σ_x and σ_y) control the degree of blurriness and hence the difficulty. Applications include removing motion blur or defocus aberration.

5.3. On-Demand Learning for Image Restoration

All three image restoration tasks offer a spectrum of difficulty. The larger the region to inpaint, the larger the percentage of deleted pixels, or the more blurry the corrupted image is, the more difficult the corresponding task. To train a system that generalizes across task difficulty, a natural approach is to simply pool training instances across all levels of difficulty, insisting that the learner simultaneously tackle all degrees of corruption at once. This parallels the learning style represented by Charlie in Sec. 1. Unfortunately, as we will see in our experiments, this approach struggles to adequately learn the concept.

Instead, we present an *on-demand* learning approach in which the system dynamically adjusts its focus where it is most needed. First, we divide each restoration task into N sub-tasks of increasing difficulty. During training, we aim to jointly train the deep neural network restoration model (architecture details below) to accommodate all N sub-tasks. Initially, we generate the same number of training examples from each sub-task in every batch. At the end of every epoch, we validate on a small validation set and evaluate the performance of the current model on all sub-tasks. We compute the mean peak signal-to-noise ratio (PSNR) for all images in the validation set for each sub-task. PSNR (higher is better) is widely used to measure image quality in image restoration tasks. A lower PSNR indicates a more difficult sub-task, suggesting that the model

needs more training on examples of this sub-task. Therefore, we generate more training examples for this sub-task in each batch in the next epoch. That is, we re-distribute the corruption levels allocated to the same set of training images. Specifically, we assign training examples in each batch for the next epoch inverse proportionally to the mean PSNR P_i of each sub-task T_i . Namely,

$$B_i = \frac{1/P_i}{\sum_{i=1}^N 1/P_i} \cdot \mathbb{B},$$

where \mathbb{B} is the batch size and B_i is the number of training examples assigned to sub-task T_i for the next epoch. We present the pseudocode of our on-demand learning algorithm as follows:

Algorithm 1: On-Demand Learning

N sub-tasks of increasing difficulty: T_1, T_2, \dots, T_N
of training examples for sub-task T_i per batch: B_i
Batch Size: \mathbb{B}
Initialization: $B_i = \mathbb{B}/N$
while not converge do
 continue training for one epoch and snapshot;
 if end of epoch then
 $i = 1$;
 for $i \leq N$ do
 validate snapshot model on sub-task T_i ;
 get mean PSNR P_i ;
 end
 update $B_i = \frac{1/P_i}{\sum_{i=1}^N 1/P_i} \cdot \mathbb{B}$;
 end
end

The number of sub-tasks N controls a trade-off between precision and run-time. Larger values of N will allow the on-demand learning algorithm more fine-grained control on its sample generation, which could lead to better results. However, the time complexity for validating on all sub-tasks at the end of each epoch is $O(N)$. Therefore, a more fine-grained division of training examples among sub-tasks comes at the cost of longer running time during training. We leave how to select the optimal value of N as future work.

On-demand learning bears some resemblance to boosting and hard negative mining, in that the system refocuses its effort on examples that were handled unsatisfactorily by the model in previous iterations of learning. However, whereas they reweight the influence given to individual (static) training samples, our idea is to self-generate *new* training instances in specified difficulty levels based on the model’s current performance.

We arrived at this simple but effective approach after investigating several other schemes inspired by curriculum

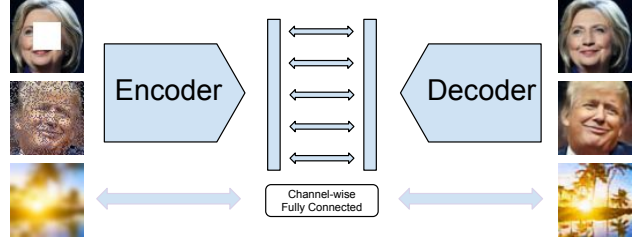


Figure 3. Network architecture for our image restoration framework. Our image restoration framework is an encoder-decoder pipeline with the encoder and decoder connected by a channel-wise fully-connected layer.

and multi-task learning that yield inferior results in practice, as we shall see below. In particular, we developed a curriculum approach that stages the training samples in order of their difficulty, starting with easier instances (less blur, smaller cut-outs) for the system to gain a basic representation, then moving onto harder ones (more blur, bigger cut-outs). Wary that what appears intuitively easier to us as algorithm designers need not be easier to the deep network, we also considered an “anti-curriculum” approach that reverses that ordering, e.g., starting with bigger missing regions for inpainting. We also designed two variants for them—staged and cumulative—which progress from difficulty level to difficulty level, or accumulate instances of increasing/decreasing difficulty, respectively. More details of these baseline methods are given in Sec. 6.3.

5.4. Deep Learning Network Architecture

Finally, we present the network architecture used for all tasks to implement our on-demand learning idea. Our image restoration network is a simple encoder-decoder pipeline. See Fig. 3. The encoder takes a corrupted image \mathcal{C} of size 64×64 as input and encodes it in the latent feature space. The decoder takes the feature representation and outputs the restored image $f(\mathcal{C}, \mathbf{w})$. Our encoder and decoder are connected through a channel-wise fully-connected layer.

Fig. 4 shows the complete network architecture. For our encoder, we use four convolutional layers. Following similar design choices in DCGAN [33], we put a batch normalization layer [14] after each convolutional layer to accelerate training and stabilize learning. The leaky rectified linear unit (LeakyReLU) activation [28, 41] is used in all layers in the encoder.

The four convolutional layers in the encoder only connect all the feature maps together, but there are no direct connections among different locations within each specific feature map. Fully-connected layers are usually used to handle this information propagation in present successful network architectures [20, 35]. In our network, the latent feature dimension is $4 \times 4 \times 512 = 8192$ for both encoder and decoder. Fully-connecting our encoder and decoder

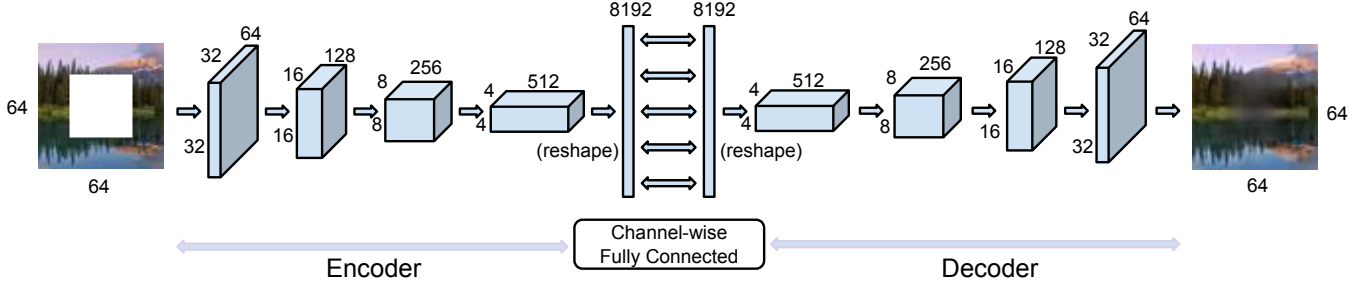


Figure 4. Network architecture for our image restoration framework. Our image restoration framework is an encoder-decoder pipeline with the encoder and decoder connected by a channel-wise fully-connected layer. The illustration is for image inpainting task. The same network architecture also holds for the other three tasks: pixel interpolation, image deblurring, and image denoising.

will increase the number of parameters explosively. To more efficiently train our network and demonstrate our concept, we use a channel-wise fully-connected layer to connect the encoder and decoder, as in [30]. The channel-wise fully-connected layer is designed to only propagate information within activations of each feature map. In our case, each 4×4 feature map in the encoder side is fully-connected with each 4×4 feature map in the decoder side. This largely reduces the number of parameters in our network and accelerates training significantly.

The decoder consists of four up-convolutional layers [27, 7, 44], each of which is followed by a rectified linear unit (ReLU) activation except the output layer. We use the Tanh function in the output layer. The series of up-convolutions and non-linearities conducts a non-linear weighted upsampling of the feature produced by the encoder and generates a higher resolution image of our target size (64×64).

The loss function we use during training is L2 loss, which is the mean squared error between the restored image $f(\mathcal{C}, \mathbf{w})$ and the real image \mathcal{R} . We use a symmetric encoder-decoder pipeline that is efficient for training and effective for learning. It is a unified framework that can be used for all four image restoration tasks.

6. Experiments

We compare our approach to both traditional “one-trick pony” learners, multi-task and curriculum methods, and several existing methods in the literature [30, 32, 1, 5, 3].

6.1. Datasets

We experiment with three datasets: CelebFaces Attributes (CelebA) [26], SUN397 Scenes [39] and Denoising Benchmark 11 (DB11) [5, 3]. We do not use any of the accompanying labels. For CelebA, we use the first 100,000 images as the training set, and the next 100,000 images as extra training data for a baseline (see Sec. 6.5). Among the rest of the images, we hold out 1,000 images each for the validation and test sets. For SUN397, similarly, we use 100,000 images for training, and 1,000 each for validation

and testing. DB11 consists of 11 standard benchmark images, such as “Lena” and “Barbara”, that have been widely used to evaluate denoising algorithms [5, 3]. We only use this dataset for our denoising case study in Sec. 6.6 to facilitate comparison with prior work.

6.2. Implementation Details

Our image restoration pipeline is implemented in Torch. We use ADAM [19] as the stochastic gradient descent solver for optimization. We use the default solver hyperparameters suggested in [33] and batch size $\mathbb{B} = 100$ in all experiments. For consistency, we divide each of the image restoration tasks into $N = 5$ difficulty levels during training. An extra level (level 6) is added during testing. The level 6 sub-task, which consists of the next interval defined uniformly as the previous N , can be regarded as an “extra credit” task that strains the generalization ability of the obtained model.

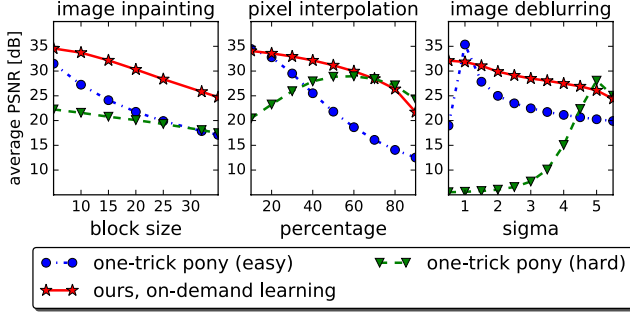
Image Inpainting: We focus on inpainting missing square blocks of size 1×1 to 30×30 at different locations across the image. We divide the range into the following five intervals, which define the five difficulty levels: $1 \times 1 - 6 \times 6$, $7 \times 7 - 12 \times 12$, $13 \times 13 - 18 \times 18$, $19 \times 19 - 24 \times 24$, $25 \times 25 - 30 \times 30$.

Pixel Interpolation: We train the pixel interpolation network with images corrupted by removing a random percentage of pixels. The percentage is sampled from the range $[0\%, 75\%]$. We divide the range into the following five difficulty levels: $0\% - 15\%$, $15\% - 30\%$, $30\% - 45\%$, $45\% - 60\%$, $60\% - 75\%$.

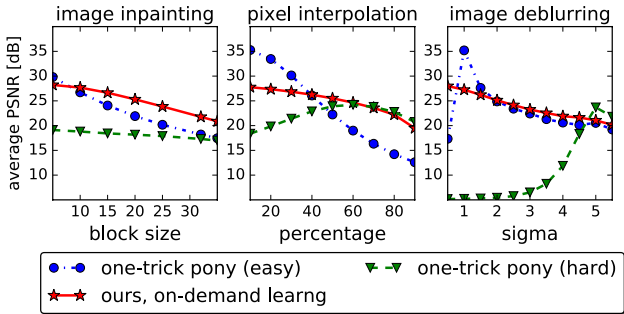
Image Deblurring: Blur kernel widths σ_x and σ_y , which are sampled from the range $[0, 5]$, control the level of difficulty. We consider the following five difficulty levels: $0 - 1$, $1 - 2$, $2 - 3$, $3 - 4$, $4 - 5$.

6.3. Baselines

For fair comparisons, all baseline models and our method are trained for the same amount of time (250



(a) Our algorithm vs. one-trick ponies on CelebA



(b) Our algorithm vs. one-trick ponies on SUN397

Figure 5. Our algorithm vs. one-trick ponies on CelebA and SUN397. Models trained using our algorithm perform well over the spectrum of difficulty, while one-trick ponies perform well at only a certain level of corruption.

epochs). Therefore, while our algorithm shifts the distribution of training instances it demands on the fly, it *never receives more training instances than the baselines*.

One-Trick Pony (Hard): Analogous to Alice in Sec. 1, the image restoration network is trained only on one corruption level of severely corrupted images.

One-Trick Pony (Easy): Analogous to Bob, the image restoration network is trained only on one corruption level of lightly corrupted images.

Rigid Joint Learning: Analogous to Charlie, the image restoration network is trained on all sub-tasks of different difficulty levels (level 1- N) jointly. We allocate the same number of training examples for each sub-task per batch.

Staged Curriculum Learning: The network starts at the easiest sub-task (level 1) and gradually switches to more difficult sub-tasks. At any time, the network trains on only one sub-task. It trains on each sub-task for 50 epochs.

Staged Anti-Curriculum Learning: The network performs as the above, but reverses the curriculum to start with the most difficult task (level N).

Cumulative Curriculum Learning: The network starts at the easiest sub-task (level 1) and gradually adds more difficult sub-tasks and learns them jointly. More specifically, the baseline model is first trained on level 1 sub-task

for 50 epochs, and then performs rigid joint learning on sub-tasks of level 1 and 2 for 50 epochs, followed by performing rigid joint learning on sub-tasks of level 1,2,3 for another 50 epochs, and so on.

Cumulative Anti-Curriculum Learning: The network performs as the above, but reverses the curriculum.

As far as source training data, the one-trick pony baselines represent the status quo in using deep learning for image restoration tasks [25, 30, 43, 40, 15, 3, 34], while the rigid joint learning baseline represents the natural solution of pooling all training data [15, 29]. The curriculum methods are of our own design. Our system never receives more training images than any baseline; only the distribution of distortions among those images evolves over epochs.

6.4. One-Trick Pony vs. All-Rounder

Fig. 6 shows qualitative examples output by our method. These illustrate that models trained using our proposed on-demand approach are all-rounders that perform well on images of different degrees of corruption. With a single model, we inpaint blocks of different sizes at arbitrary locations, restore corrupted images with different percentage of deleted pixels, and deblur images at various degrees of blurriness. Please see Fig. 10 for more qualitative examples.

We next show that our on-demand learning algorithm successfully addresses the one-trick pony problem, where the one-trick ponies employ an identical network architecture to ours. For inpainting, the one-trick pony (hard/easy) is only trained to inpaint 32×32 or 5×5 central blocks, respectively; for pixel interpolation, 80% (hard) or 10% (easy) pixels are deleted; for deblurring, $\sigma_x = \sigma_y = 5$ (hard) or $\sigma_x = \sigma_y = 1$ (easy).

Fig. 5 summarizes the test results on images of various corruption levels. One-trick pony overfits to a specific corruption level (easy or hard). It succeeds beautifully for images within its specialty (see Fig. 2 and Fig. 9), but performs poorly when forced to attempt instances outside its specialty. In contrast, models trained using our algorithm perform well across the spectrum of difficulty. For inpainting, the one-trick ponies even perform poorly at the size they specialize in, because they also overfit to the central location, thus unable to inpaint satisfactorily at random locations at test time.

We also compare our image inpainter against a state-of-the-art inpainter from Pathak *et al.* [30]. We adapt their provided code² and follow the same procedures as in [30] to train two variants on CelebA: one is only trained to inpaint central square blocks, and the other is trained to inpaint regions of arbitrary shapes. Table 2 compares both variants to our model on the held out CelebA test set. Their first inpainter performs very well when testing on central square

²<https://github.com/pathak22/context-encoder>

	CelebA						SUN397					
	Image Deblurring		Pixel Interpolation		Image Inpainting		Image Deblurring		Pixel Interpolation		Image Inpainting	
	L2 Loss	PSNR	L2 Loss	PSNR	L2 Loss	PSNR	L2 Loss	PSNR	L2 loss	PSNR	L2 Loss	PSNR
Rigid Joint Learning	1.92	28.25 dB	1.21	30.69 dB	1.33	30.57 dB	4.77	24.34 dB	3.08	26.52 dB	2.79	27.57 dB
Cumulative Curriculum	2.17	27.84 dB	1.29	30.57 dB	1.65	29.82 dB	5.19	23.96 dB	3.22	26.41 dB	3.07	27.13 dB
Cumulative Anti-Curriculum	1.82	28.26 dB	1.19	30.78 dB	1.31	30.48 dB	4.79	24.01 dB	3.02	26.59 dB	2.82	27.42 dB
Staged Curriculum	84.7	16.87 dB	1.87	28.20 dB	1.50	29.69 dB	110	14.10 dB	5.31	23.80 dB	3.14	26.71 dB
Staged Anti-Curriculum	5.55	24.96 dB	8.41	26.57 dB	4.98	27.16 dB	9.07	22.20 dB	8.43	24.38 dB	5.71	25.51 dB
On-Demand Learning	1.75	28.56 dB	1.13	30.89 dB	1.32	30.52 dB	4.60	24.54 dB	2.95	26.78 dB	2.75	27.60 dB

Table 1. Summary of the overall performance of all algorithms for the three image restoration tasks on the CelebA and SUN397 datasets. Overall performance is measured by the mean L2 loss (in %, lower is better) and mean PSNR (higher is better) averaged over all sub-tasks. Numbers are obtained over 20 trials with standard error (SE) approximately 5×10^{-6} for L2 loss and 2×10^{-3} for PSNR on average.

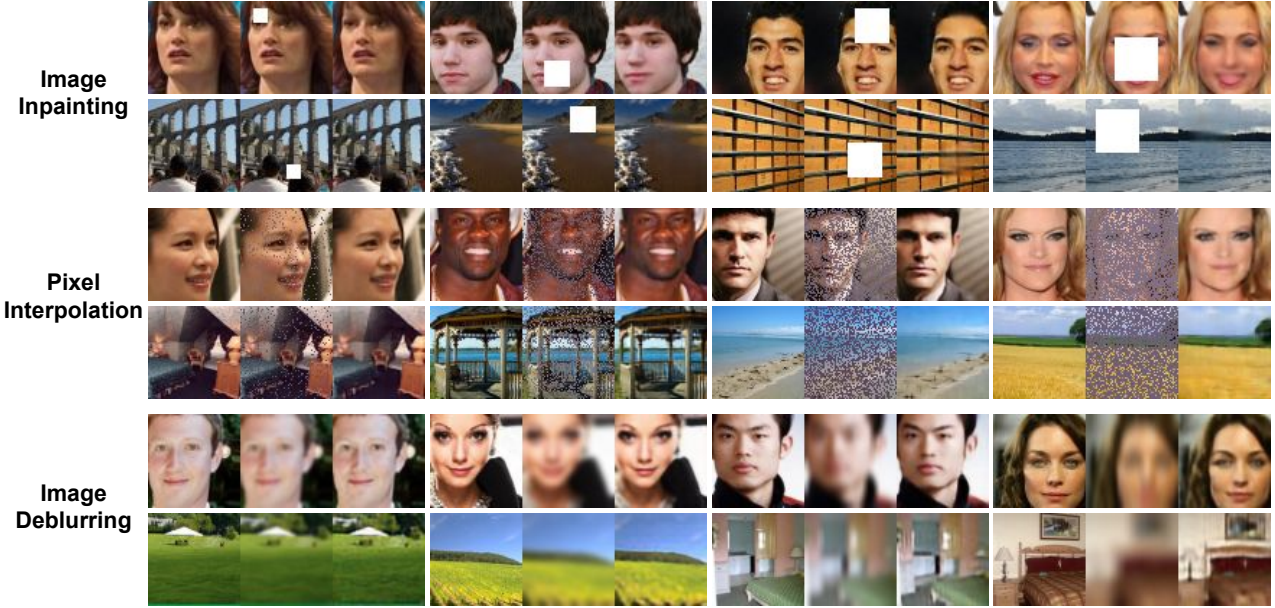


Figure 6. For each task, the first row shows testing examples of CelebA dataset, and the second row shows examples of SUN397 dataset. For each triple, **Column 1**: Original image from the dataset; **Column 2**: Corrupted image; **Column 3**: Restored image using our method. The all-rounder models trained using our proposed algorithm perform well on images with various corruption levels.

blocks (left cols), but it is unable to produce satisfactory results when tested on square blocks located anywhere in the image (right cols). The “all-rounder” inpainter trained under our on-demand learning framework does similarly well in both cases. It is competitive—and stronger on the more difficult task—even without the use of adversarial loss as used in their framework during training.

Method	Central Square Block		Arbitrary Square Block	
	L2 Loss	PSNR	L2 Loss	PSNR
Pathak <i>et al.</i> [30] Center	0.83%	22.16 dB	6.84%	11.80 dB
Pathak <i>et al.</i> [30] Random	2.47%	16.18 dB	2.51%	16.20 dB
Ours	0.93%	20.74 dB	1.04%	20.31 dB

Table 2. Image inpainting accuracy for CelebA on test set.

6.5. All-Rounder vs. Alternative Models

We next compare our method to the curriculum and multi-task baselines. Table 1 shows the results. We report average L2 loss and PSNR over all test images to summarize the results. Our proposed algorithm consistently out-

performs the well-designed baselines. The Staged (Anti-)Curriculum Learning algorithms overfit to the last sub-task they are trained on, yielding inferior overall performance. The Cumulative (Anti-)Curriculum Learning algorithms and Rigid Joint Learning are more competitive, because they learn sub-tasks jointly and try to perform well on sub-tasks across all difficulty levels. Note that for inpainting, we help the baselines by randomizing the locations of inpainting blocks, which partially solves the one-trick pony problem. Therefore, some baselines can perform similarly to ours on image inpainting. Nevertheless, by automatically guiding the balance among sub-tasks, our algorithm obtains the best all-around performance. On average, our algorithm has about 15% relative advantage over all our baselines in terms of PSNR.

We argue that the gain of our algorithm does not rest on *more* training instances of certain sub-tasks, but rather a suitable combination of sub-tasks for effective training. Indeed, we never use more training instances than any base-

Image	GSM [32]	KSVD [1]	BM3D [5]	MLP [3]	Ours
Barbara	27.83 dB	29.49 dB	30.67 dB	29.21 dB	27.96 dB
Boat	29.29 dB	29.24 dB	29.86 dB	29.89 dB	30.00 dB
C.man	28.64 dB	28.64 dB	29.40 dB	29.32 dB	29.10 dB
Couple	28.94 dB	28.87 dB	29.68 dB	29.70 dB	29.92 dB
F.print	27.13 dB	27.24 dB	27.72 dB	27.50 dB	27.79 dB
Hill	29.26 dB	29.20 dB	29.81 dB	29.82 dB	29.98 dB
House	31.60 dB	32.08 dB	32.92 dB	32.50 dB	33.00 dB
Lena	31.25 dB	31.30 dB	32.04 dB	32.12 dB	32.37 dB
Man	29.16 dB	29.08 dB	29.58 dB	29.81 dB	29.82 dB
Montage	30.73 dB	30.91 dB	32.24 dB	31.85 dB	31.91 dB
Peppers	29.49 dB	29.69 dB	30.18 dB	30.25 dB	30.06 dB

Table 3. PSNRs (higher is better) on standard test images, $\sigma = 25$

line. To emphasize this point, after running our method and rigid joint training to convergence, we then *only* give the baseline 100,000 *extra* training images from CelebA to continue its training.³ We observe that the extra training instances do not help rigid joint training converge to a better local minimum. This preliminary results suggest on-demand learning’s gains persist *even if our method is put at the disadvantage of having access to 50% fewer novel training images*.

How does the system focus its attention as it learns? To get a sense, we examine the learned allocation of sub-tasks during training. Initially, each sub-task is assigned the same number of training instances per batch. In all tasks, as training continues, the network tends to dynamically shift its allocations to put more emphasis on the “harder” sub-tasks, while never abandoning the “easiest” ones.

6.6. Comparison to Existing Denoising Methods

Image denoising is a classic image restoration problem widely studied in the literature [32, 1, 5, 3, 29]. In this section, we perform a case study on the image denoising task using our framework. We train a denoising network using SUN397 images and the same architecture described in Sec. 5.4, except that the input and output are grayscale images. We corrupt the real image \mathcal{R} by adding additive white Gaussian (AWG) noise with standard deviation σ to synthesize our training data. The five sub-tasks are defined by sampling σ from the following five ranges: 0 – 20, 20 – 40, 40 – 60, 60 – 80, 80 – 100. Because the input of our network is of size 64×64 , given a larger corrupted image \mathcal{C} , we first decompose the image into overlapping patches of size 64×64 and use a sliding-window approach to denoise each patch separately (stride 3 pixels), then average outputs at overlapping pixels.

We test our image denoising system on DB11 [5, 3]. We first compare our model with state-of-the-art denoising algorithms on images with a specific degree of corruption ($\sigma = 25$, commonly adopted to train one-trick ponies in the literature). Table 3 summarizes the results⁴. Although our

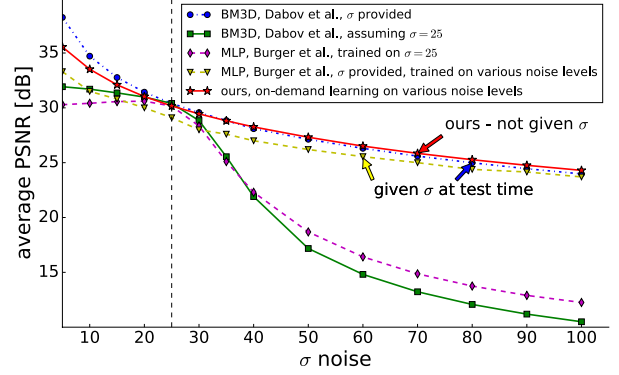


Figure 7. Comparisons of the performance of image denoising systems at different noise levels. Our system is competitive over the whole spectrum of noise levels without requiring knowledge of the corruption level of test images. Best viewed in color.

model does not specialize in this level of corruption, we still have very competitive performance. We outperform all four existing denoising algorithms on 7 out of the 11 test images.

More importantly, the advantage of our method is more apparent when we test across the spectrum of difficulty levels. We corrupt the DB11 images with AWG noise of increasing magnitude and compare with the state-of-the-art denoising algorithms BM3D [5] and MLP [3] based on the authors’ public code⁵⁶ and reported results [3]. We compare with two MLP models: one is trained only on corrupted images of $\sigma = 25$, and the other is trained on images with various noise levels. BM3D and MLP both need to be provided with the correct level of the noise (σ) during testing. We also run a variant of BM3D for different noise levels but fix the specified level of noise to $\sigma = 25$.

Fig. 7 shows the results. We see that the MLP model [3] trained on a single noise level only performs well at that specific level of corruption. Similarly, BM3D [5] needs the correct input of noise level in order to perform well across the spectrum of noise levels. In contrast, our image denoising system consistently performs well on all noise levels, yet we *do not* assume knowledge of σ during testing. This is an essential advantage for real-world applications.

Finally, we show some qualitative results of our image denoising system. Particularly, we first compare the denoising results of image Lena across the spectrum of difficulty in Fig. 8. We show image denoising results at four different corruption levels ($\sigma = 10, 25, 50, 75$). For each row, the first column shows the original real image; the second column shows the image corrupted by AWG noise with the specified sigma value; the third column shows the restoration result using BM3D [5] assuming $\sigma = 25$ for the test image; the

our image denoising system for comparison.

⁵<http://www.cs.tut.fi/~foi/GCF-BM3D/>

⁶http://people.tuebingen.mpg.de/burger/neural_denoising/

³The other datasets lack sufficient data to run this test.

⁴We take the reported numbers from [3] and add the performance of

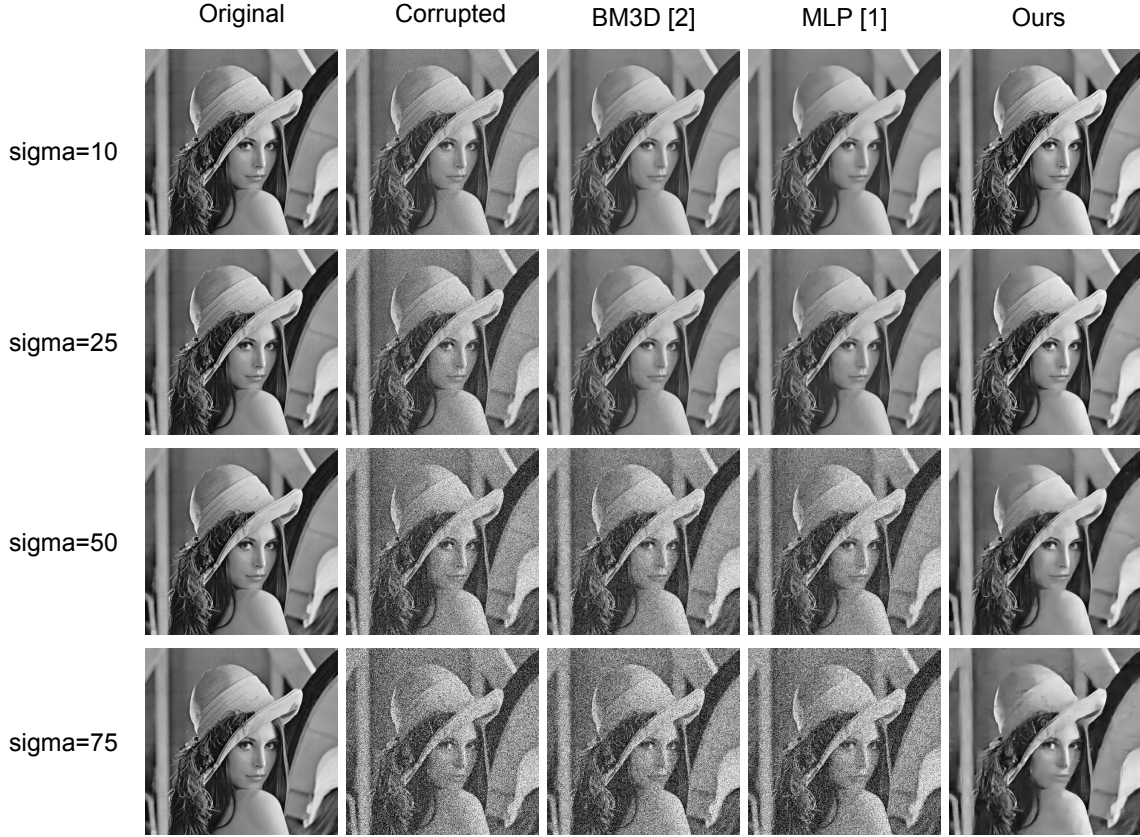


Figure 8. Denoising results of image Lena at various corruption levels. For each row, **Column 1**: Original image from the dataset; **Column 2**: Corrupted image of specified sigma value; **Column 3**: Restored image using BM3D [5] assuming $\sigma = 25$ for all corrupted images; **Column 4**: Restored image using MLP [3] trained for $\sigma = 25$; **Column 5**: Restored image using our image denoising system. All methods are applied as a single model to all test images. BM3D [5] and MLP [3] perform well only at a particular level of corruption, while the image denoising model trained using our method performs well at all corruption levels.

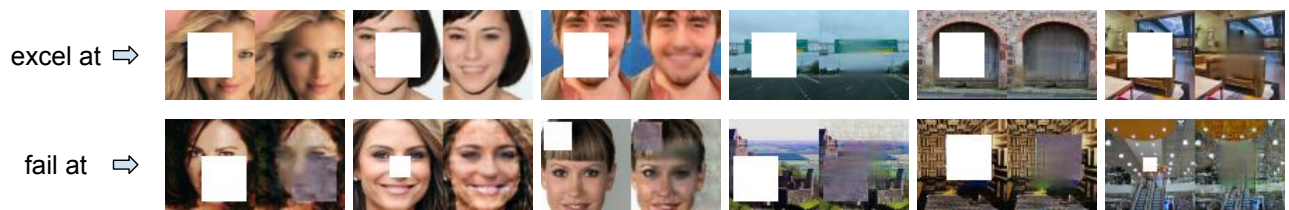
fourth column shows the denoising result of the MLP [3] model trained for $\sigma = 25$ ⁷; the last column shows the denoising result of the model trained using our on-demand learning algorithm. BM3D only works well when given the correct sigma value at test time, which is impractical because it is difficult to gauge the corruption level in a novel image and decide which sigma value to use. The MLP model trained for $\sigma = 25$ is a one-trick pony that performs well only at that specific level of corruption. However, the model trained using our proposed method performs well on all four corruption levels, and it is a single model without knowing the correct sigma value of corrupted images at test time. In the end of the paper, we also append the image denoising results using our denoising system of all the 11

images at noisy level $\sigma = 25$.

7. Conclusion

We have addressed a common problem in existing work that leverages deep models to solve image restoration tasks: the one-trick pony. We propose a simple but novel *on-demand learning* algorithm that turns a one-trick pony into an all-rounder that performs well on a task across the spectrum of difficulty. Experiments on four image restoration tasks on three diverse datasets demonstrate the effectiveness of our method. Our on-demand learning idea is a general concept not restricted to image restoration tasks, and may be applicable in other domains as well, e.g., self-supervised feature learning. As future work, we plan to design continuous sub-tasks to avoid discrete sub-task bins, and we will explore ways to make an image restoration task more self-paced by allowing the network to design the most desired sub-task on its own. Finally, another promising direction is to discover an all-rounder model for combinations of different types of distortions.

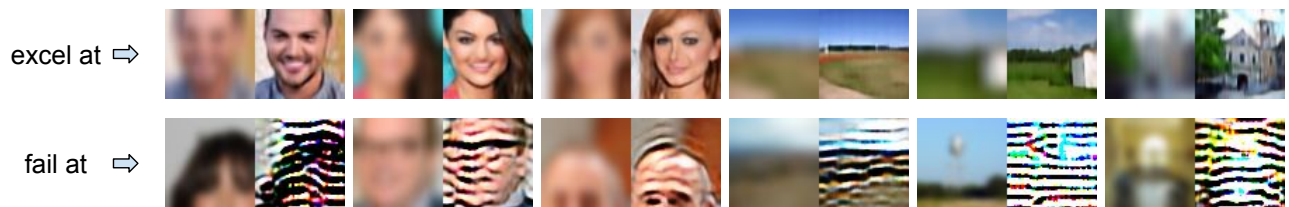
⁷We use the authors publicly available code (http://people.tuebingen.mpg.de/burger/neural_denoising/) in which the system is trained for $\sigma = 25$. The authors also propose a variant of the system trained on various corruption levels with σ given as input to the network, and it requires the σ value to be available at test time. This version is not available in the public code, and it is also unclear how the true σ value would be available for a novel image with unknown distortions.



(a) one-trick pony for image inpainting task



(b) one-trick pony for pixel interpolation task



(c) one-trick pony for image deblurring task

Figure 9. More qualitative examples of One-Trick Ponies for image inpainting, pixel interpolation, and image deblurring tasks. The models overfit to a certain degree of corruption. They perform extremely well at that level of corruption, yet fail to produce satisfactory restoration results even for much easier sub-tasks.

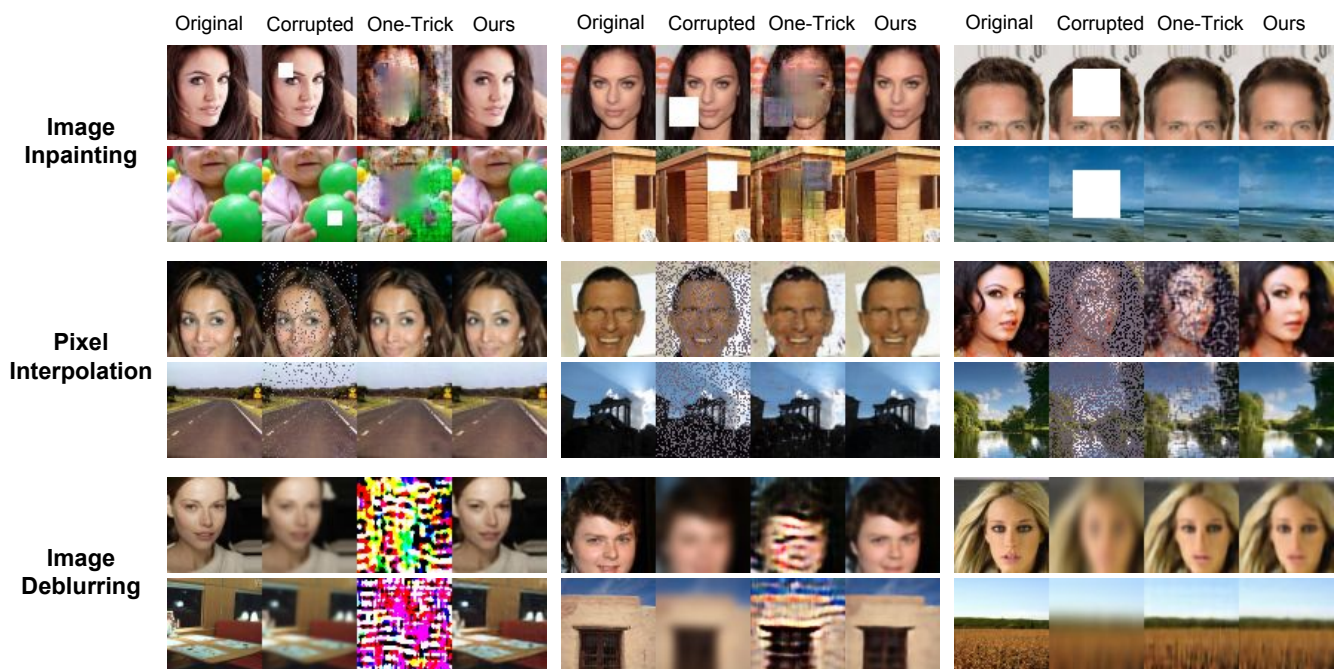
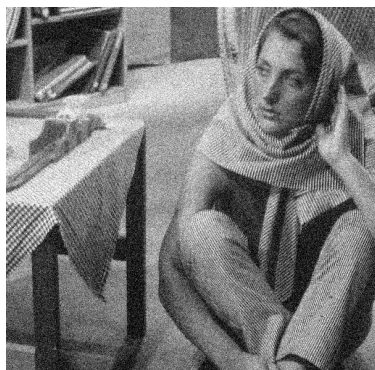


Figure 10. More qualitative examples of image restoration results of all-rounder models trained using our proposed on-demand learning algorithm. For each task, the first row shows testing examples of CelebA dataset, and the second row shows examples of SUN397 dataset. For each quadruple, **Column 1**: Original image from the dataset; **Column 2**: Corrupted image; **Column 3**: Restored image using a one-trick pony model; **Column 4**: Restored image using our method. Models trained using our method can handle arbitrary levels of distortions, while the one-trick pony models can only perform well at a particular level of corruption.



clean (name: Barbara)



noisy (PSNR: 20.28 dB)



ours (PSNR: 27.96 dB)



clean (name: Boat)



noisy (PSNR: 20.29 dB)



ours (PSNR: 30.00 dB)



clean (name: C.man)



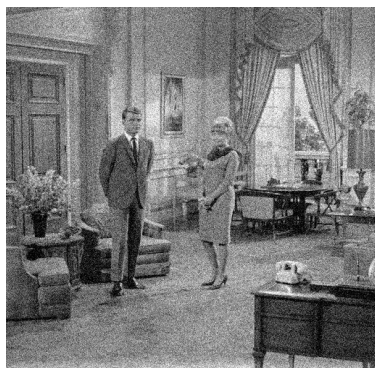
noisy (PSNR: 20.60 dB)



ours (PSNR: 29.10 dB)



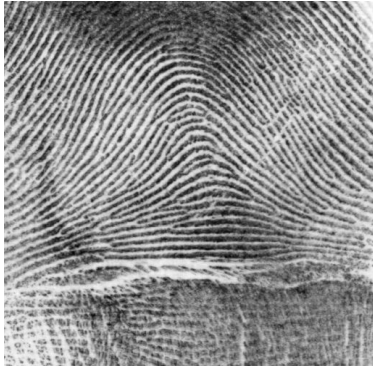
clean (name: Couple)



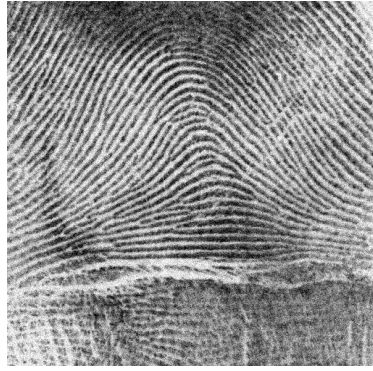
noisy (PSNR: 20.28 dB)



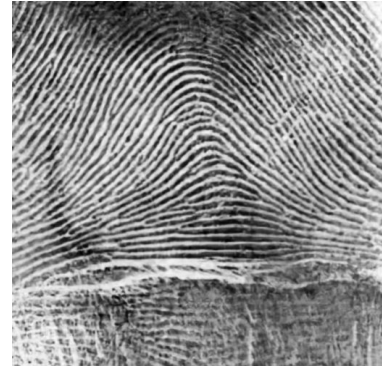
ours (PSNR: 29.92 dB)



clean (name: F.print)



noisy (PSNR: 20.29 dB)



ours (PSNR: 27.79 dB)



clean (name: Hill)



noisy (PSNR: 20.28 dB)



ours (PSNR: 29.98 dB)



clean (name: House)



noisy (PSNR: 20.22 dB)



ours (PSNR: 33.00 dB)



clean (name: Lena)



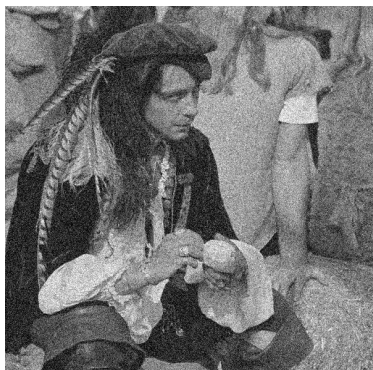
noisy (PSNR: 20.24 dB)



ours (PSNR: 32.37 dB)



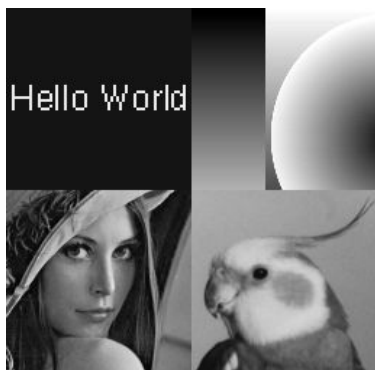
clean (name: Man)



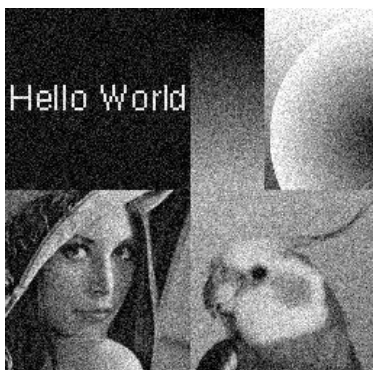
noisy (PSNR: 20.24 dB)



ours (PSNR: 29.82 dB)



clean (name: Montage)



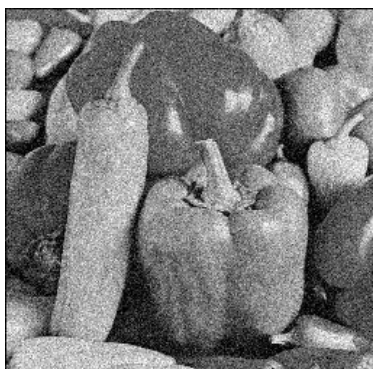
noisy (PSNR: 20.77 dB)



ours (PSNR: 31.91 dB)



clean (name: Peppers)



noisy (PSNR: 20.31 dB)



ours (PSNR: 30.06 dB)

References

- [1] M. Aharon, M. Elad, and A. Bruckstein. K-svd: An algorithm for designing overcomplete dictionaries for sparse representation. *IEEE Transactions on signal processing*, 2006. 6, 9
- [2] Y. Bengio, J. Louradour, R. Collobert, and J. Weston. Curriculum learning. In *ICML*, 2009. 2
- [3] H. C. Burger, C. J. Schuler, and S. Harmeling. Image denoising: Can plain neural networks compete with bm3d? In *CVPR*, 2012. 2, 3, 6, 7, 9, 10
- [4] D. Cho, Y.-W. Tai, and I. Kweon. Natural image matting using deep convolutional neural networks. In *ECCV*, 2016. 1, 2
- [5] K. Dabov, A. Foi, V. Katkovnik, and K. Egiazarian. Image denoising by sparse 3-d transform-domain collaborative filtering. *IEEE Transactions on image processing*, 2007. 2, 6, 9, 10
- [6] C. Dong, C. C. Loy, K. He, and X. Tang. Image super-resolution using deep convolutional networks. *TPAMI*, 2016. 1, 2
- [7] A. Dosovitskiy, J. Tobias Springenberg, and T. Brox. Learning to generate chairs with convolutional neural networks. In *CVPR*, 2015. 6
- [8] D. Eigen, D. Krishnan, and R. Fergus. Restoring an image taken through a window covered with dirt or rain. In *CVPR*, 2013. 2
- [9] E. Elhamifar, G. Sapiro, A. Yang, and S. Shankar Sasrty. A convex optimization framework for active learning. In *ICCV*, 2013. 3
- [10] J. L. Elman. Learning and development in neural networks: The importance of starting small. *Cognition*, 1993. 2
- [11] A. Freytag, E. Rodner, and J. Denzler. Selecting influential examples: Active learning with expected model output changes. In *ECCV*, 2014. 3
- [12] K. He, X. Zhang, S. Ren, and J. Sun. Deep residual learning for image recognition. In *CVPR*, 2016. 1
- [13] S.-J. Huang, R. Jin, and Z.-H. Zhou. Active learning by querying informative and representative examples. *TPAMI*, 2014. 3
- [14] S. Ioffe and C. Szegedy. Batch normalization: Accelerating deep network training by reducing internal covariate shift. *arXiv preprint arXiv:1502.03167*, 2015. 5
- [15] V. Jain and S. Seung. Natural image denoising with convolutional networks. In *NIPS*, 2009. 2, 7
- [16] J. Johnson, A. Alahi, and L. Fei-Fei. Perceptual losses for real-time style transfer and super-resolution. *ECCV*, 2016. 1, 2
- [17] C. Käding, A. Freytag, E. Rodner, P. Bodesheim, and J. Denzler. Active learning and discovery of object categories in the presence of unnameable instances. In *CVPR*, 2015. 3
- [18] A. Kapoor, K. Grauman, R. Urtasun, and T. Darrell. Gaussian processes for object categorization. *IJCV*, 2010. 3
- [19] D. Kingma and J. Ba. Adam: A method for stochastic optimization. *ICLR*, 2015. 6
- [20] A. Krizhevsky, I. Sutskever, and G. E. Hinton. Imagenet classification with deep convolutional neural networks. In *NIPS*, 2012. 1, 5
- [21] M. P. Kumar, B. Packer, and D. Koller. Self-paced learning for latent variable models. In *NIPS*, 2010. 2
- [22] G. Larsson, M. Maire, and G. Shakhnarovich. Learning representations for automatic colorization. *ECCV*, 2016. 1, 2
- [23] Y. J. Lee and K. Grauman. Learning the easy things first: Self-paced visual category discovery. In *CVPR*, 2011. 2
- [24] X. Li and Y. Guo. Multi-level adaptive active learning for scene classification. In *ECCV*, 2014. 3
- [25] S. Liu, J. Pan, and M.-H. Yang. Learning recursive filters for low-level vision via a hybrid neural network. In *ECCV*, 2016. 1, 2, 3, 7
- [26] Z. Liu, P. Luo, X. Wang, and X. Tang. Deep learning face attributes in the wild. In *ICCV*, 2015. 2, 6
- [27] J. Long, E. Shelhamer, and T. Darrell. Fully convolutional networks for semantic segmentation. In *CVPR*, 2015. 6
- [28] A. L. Maas, A. Y. Hannun, and A. Y. Ng. Rectifier nonlinearities improve neural network acoustic models. In *ICML*, 2013. 5
- [29] X.-J. Mao, C. Shen, and Y.-B. Yang. Image restoration using very deep convolutional encoder-decoder networks with symmetric skip connections. *NIPS*, 2016. 2, 7, 9
- [30] D. Pathak, P. Krahenbuhl, J. Donahue, T. Darrell, and A. A. Efros. Context encoders: Feature learning by inpainting. In *CVPR*, 2016. 1, 2, 3, 4, 6, 7, 8
- [31] A. Pentina, V. Sharmanska, and C. H. Lampert. Curriculum learning of multiple tasks. In *CVPR*, 2015. 2
- [32] J. Portilla, V. Strela, M. J. Wainwright, and E. P. Simoncelli. Image denoising using scale mixtures of gaussians in the wavelet domain. *IEEE Transactions on Image processing*, 2003. 6, 9
- [33] A. Radford, L. Metz, and S. Chintala. Unsupervised representation learning with deep convolutional generative adversarial networks. In *ICLR*, 2016. 5, 6
- [34] C. J. Schuler, H. Christopher Burger, S. Harmeling, and B. Scholkopf. A machine learning approach for non-blind image deconvolution. In *CVPR*, 2013. 2, 3, 7
- [35] K. Simonyan and A. Zisserman. Very deep convolutional networks for large-scale image recognition. In *ICLR*, 2015. 1, 5
- [36] S. Vijayanarasimhan and K. Grauman. Large-scale live active learning: Training object detectors with crawled data and crowds. *IJCV*, 2014. 3
- [37] P. Vincent, H. Larochelle, Y. Bengio, and P.-A. Manzagol. Extracting and composing robust features with denoising autoencoders. In *ICML*, 2008. 2
- [38] Z. Wang, B. Du, L. Zhang, L. Zhang, M. Fang, and D. Tao. Multi-label active learning based on maximum correntropy criterion: Towards robust and discriminative labeling. In *ECCV*, 2016. 3
- [39] J. Xiao, K. A. Ehinger, J. Hays, A. Torralba, and A. Oliva. Sun database: Exploring a large collection of scene categories. *IJCV*, 2014. 2, 6
- [40] J. Xie, L. Xu, and E. Chen. Image denoising and inpainting with deep neural networks. In *NIPS*, 2012. 2, 3, 7
- [41] B. Xu, N. Wang, T. Chen, and M. Li. Empirical evaluation of rectified activations in convolutional network. *arXiv preprint arXiv:1505.00853*, 2015. 5

- [42] L. Xu, J. S. Ren, C. Liu, and J. Jia. Deep convolutional neural network for image deconvolution. In *NIPS*, 2014. 2
- [43] R. Yeh, C. Chen, T. Y. Lim, M. Hasegawa-Johnson, and M. N. Do. Semantic image inpainting with perceptual and contextual losses. *arXiv preprint arXiv:1607.07539*, 2016. 1, 2, 3, 4, 7
- [44] M. D. Zeiler and R. Fergus. Visualizing and understanding convolutional networks. In *ECCV*, 2014. 6
- [45] R. Zhang, P. Isola, and A. A. Efros. Colorful image colorization. *ECCV*, 2016. 1, 2